UWB Positioning System with the Support of MEMS Sensors for Indoor and Outdoor Environment

Krzysztof Paszek, Damian Grzechca, Mateusz Tomczyk, and Artur Marciniak
Faculty of Automatic Control, Electronics and Computer Science
Silesian University of Technology, Gliwice 44-100, Poland
Email: {Krzysztof.Paszek, Damian.Grzechca}@polsl.pl; {matetom094, artumar212}@student.polsl.pl

Abstract —Positioning systems should depend on a number of sub-systems such as global positioning system (GPS), inertial navigation system (INS), lidar, radar, vision systems etc. due to the growing popularity of autonomous vehicles. High accuracy of positioning process must be included due to driving safety (of autonomous vehicles and drivers in vehicles with assistance systems). The paper investigates the movement of a radio-controlled (RC) model. The article presents the process of fusion and filtration on data from ultra-wideband (UWB) and INS systems. It focuses on the error that occurs in the first phase of determining a position, namely when the distance between two nodes is calculated. This error affects further process of data – trilateration, which is the next step to determine the position of objects. A method of data correction based on system information obtained from static measurements is also presented. The tests were carried out both indoors and outdoors, which illustrates the variability of the problem depending on the environment. Reference data for dynamic tests were obtained from a single-stripe lidar.

Index Terms—UWB, indoor/outdoor positioning, MEMS, lidar, filters

I. Introduction

Many technologies are used to position objects indoors and outdoors [1], [2]. Each of them has advantages and disadvantages that should be eliminated by proper data analysis and/or by merging with data from different positioning subsystems [3], [4].

In critical applications, various types of systems are multiplicated to increase the reliability and safety. Safety should be ensured not only at the hardware level but also at the software level [5]. In autonomous vehicles, one of the most important goals, is to prepare the system so that the passage of the vehicle is as safe for a driver, passengers and all other road users as possible. To ensure this level of safety, it is necessary to achieve the most accurate position of the object and obtain as much information about other objects around the vehicle as possible.

Many positioning subsystems should be considered in the positioning process and all their advantages should be used to eliminate all disadvantages of individual systems for this purpose. The drawback of a particular positioning technology may be e.g. the range of the system, costs or failure to operate under certain conditions (e.g. weather conditions, indoors).

Technologies widely used in positioning, autonomous vehicles or advanced driver assistance systems (ADAS) include among others: lidar [6], [7], radar [8], Wi-Fi [9], Bluetooth [10], global positioning system (GPS) [11], inertial navigation system (INS) using micro electro-mechanical systems (MEMS) sensors [12], ultrasound [13] and camera vision systems [14]. Information from many positioning subsystems allows to analyse the area in the immediate neighbourhood of a moving vehicle and over greater distances.

Multi-stripe lidars or long-range and short-range radars are used in vehicles mainly to detect other traffic participants (e.g. pedestrians, other vehicles) or elements of infrastructure. Furthermore, it is possible to safely avoid collision, perform emergency braking (while the driver's response is too slow or it is not happening at all), and keep a safe distance between vehicles, e.g. in Adaptive Cruise Control (ACC) [15].

A camera vision system allows to observe the immediate surroundings of the object. It is responsible for detecting vertical and horizontal traffic signs, and road surface markings (their analysis allows, for example, to adjust the speed to the current speed limit on a given stretch of the road), detecting the lane [16], or assisting the driver during parking (displaying the area behind the vehicle on the console).

Ultrasonic sensors are mainly used to assist a driver during parking by warning about coming to an obstacle. This system can alert drivers of objects in front of and behind the vehicle.

GPS allows you to locate an object in a global system, which makes it possible to plot positions on the map [17]. After correlating global position data with the corresponding point on the map, you can obtain additional information about fixed elements of the road infrastructure.

This article presents the use of a system based on ultra-wideband (UWB) technology to determine the position of the objects indoors or as a support system in areas that require high positioning accuracy and additional communication between traffic participants or

Manuscript received October 18, 2019; revised May 5, 2020.
This work was supported by the Ministry of Science and Higher Education of Poland funding for statutory activities (BKMN2019).
Corresponding author email: Krzysztof.Paszek@polsl.pl.
doi:10. 12720/jcm.15.6.511-518

infrastructure elements (e.g. intersections, railroad crossings, tunnels). The first error in determining the position of objects is generated when the individual distances between the positioned object and selected anchors in the network are calculated [18]. This error affects the determined position in the trilateration process [19]. Therefore, this article focuses on increasing the accuracy of the distance between two individual nodes in the network (black part of Fig. 1).

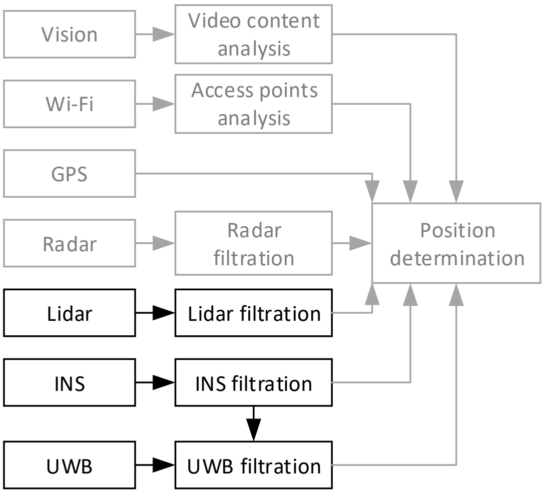

Fig. 1. System architecture.

The system based on UWB technology used indoors (e.g. production halls, warehouse, underground car parks, tunnels) allows to place the object's position on the building plan at a low cost [20]. Once built, the network infrastructure (UWB anchor network) can manage many moving objects; there is only one requirement, the UWB marker must be placed on the new object. This system is an alternative to the GPS, which is commonly used outdoors and does not work indoors. In addition, the positioning accuracy of objects using UWB technology is higher compared to GPS [21]. Therefore, this technology can increase positioning accuracy also outside buildings, at sensitive points (areas) where accuracy of the determined position is crucial and also in the areas where the GPS position is not available e.g. tunnels or underground parking. The possibility of sending additional data between UWB nodes allows communication between moving objects, and/or road infrastructure or even broadcasting information and road warnings (e.g. about accidents or traffic congestion). UWB technology can also support camera vision systems during traffic signs recognition. A sign equipped with a UWB node can broadcast information about its character.

Systems that use additional technology for positioning objects, can not only increase the accuracy of the position, but also enable to build a more universal system and thus safer. Thanks to this, it is possible to avoid collisions with other traffic participants or road infrastructure elements, adjust the speed to applicable restrictions, warn about an object in the blind spot, or assist drivers during parking.

II. TESTS

A. Test Stand

The test stand aims to collect data that allows to examine the accuracy of ranging between two UWB nodes. The stand includes:

- radio-controlled (RC) model - a vehicle remotely controlled by a man using 2.4 GHz remote controller, which allows to smoothly regulate the speed and steering of the wheels. Fully adjustable suspension – both toe-in and camber, allows for a straight drive on a flat surface without making unnecessary adjustments by turning the wheels. The model is equipped with a UWB tag, lidar, smartphone and Raspberry Pi – see Fig. 2;

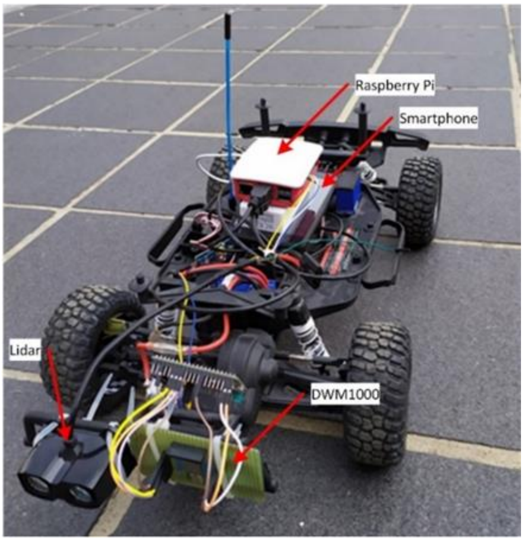

Fig. 2. Measuring platform.

- UWB node – a wireless network device using UWB technology. Decawave DWM1000 modules were used. The accuracy declared by the manufacturer is 10 cm. Sampling frequency 100 Hz. A microcontroller (STM32F103C8T6) from the STM32 MCU family is responsible for sending and receiving data from and to the node, and for communication with the Raspberry Pi;
- Lidar – a device that uses laser light pulses to scan the environment. The signal time-of-flight (ToF) is used to determine the distance. This time corresponds with the distance that the light pulse travels from the transmitter, then reflects from the object and returns to the receiver. Knowing the speed of light and half of the ToF, it is possible to determine the distance between the transmitter and the point from which the signal was reflected. The research used an optical distance sensor – Garmin LIDAR-Lite v3HP, which has a single-stripe class 1 laser in accordance with EN/IEC 60825-1 2014. The measuring range is 40 m, resolution ± 1 cm, accuracy ± 2 cm (when the distance is less than 2 m the accuracy is ± 5cm), frequency above 200 Hz;

- Smartphone – a device equipped with IMU (inertial measurement unit) sensors, thanks to the accelerometer the state of the movement of the object is detected (acceleration, braking, uniform motion etc.). The Sony Xperia Z3 smartphone was used in the research;
- Raspberry Pi – a minicomputer that acquires data from all subsystems (smartphone, lidar) and records them on an SD card.

B. Test Scenarios

Tests were carried out indoors and outdoors. Two different types of passage were made for both environments:

- smooth passage – the vehicle started to move and after 18 m of smooth driving stopped – see Fig. 3;

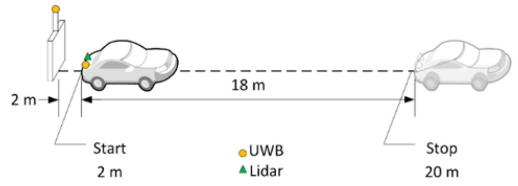

Fig. 3. 18 m smooth passage without additional stops.

- Start-stop passage – the vehicle travelled the same path as in first scenario, but stopped at three checkpoints after driving 3 m, 8 m and 13 m – see Fig. 4;

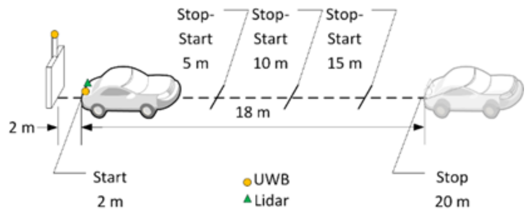

Fig. 4. 18 m passage with three additional stops.

C. Distance Calculation

The asymmetrical double-sided two-way ranging (ADS-TWR) algorithm was used to determine the distance between two UWB nodes [22]. This algorithm uses 3 messages to determine the propagation time of the signal – t_{prop} (1). The algorithm is denoted as asymmetrical, because there is no need for response times on both devices to be the same, which directly translate into better results and a small error.

$$t_{prop} = \frac{t_{round_1} \cdot t_{round_2} - t_{reply_1} \cdot t_{reply_2}}{t_{round_1} + t_{round_2} + t_{reply_1} + t_{reply_2}} \quad (1)$$

where: t_{round} – time from sending a message to receiving the response; t_{reply} – time from receiving the message to sending a response.

III. Analysis and Filtration of Data

The reference data (distances) obtained from lidar was filtered with a second order Savitzky-Golay (SG) [23] filter with a window size of 13 samples, to eliminate random measurement errors and noise from the data. Fig. 5 presents raw ($Lidar_{RAW}$) and filtered data from lidar ($Lidar_{SG}$), for example, of an indoor passage.

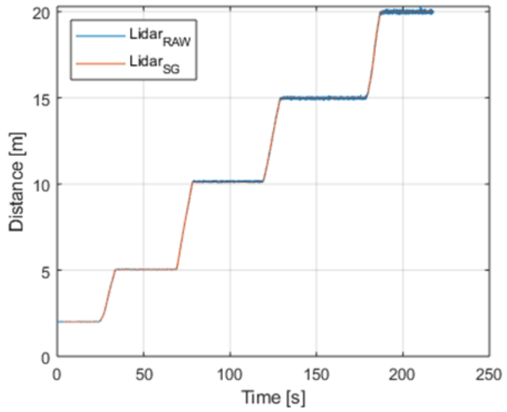

Fig. 5. Example of passage indoor, raw and filtered data of lidar.

As the distance increases the data from the lidar are becoming noisier – it is notably visible when the vehicle is not moving (horizontal line). Fig. 6 shows a fragment of the previously presented passage, where the data was smoothed while maintaining the sharpness of the flow.

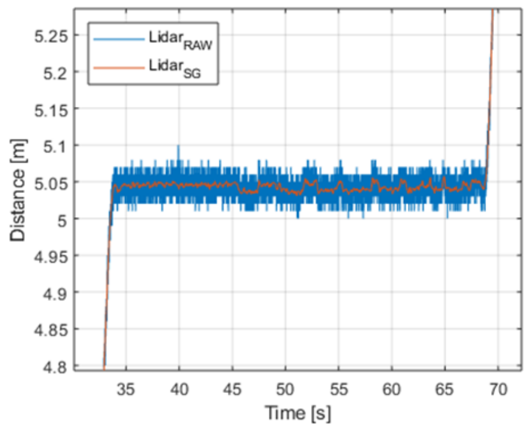

Fig. 6. Lidar data after Savitzky-Golay filtering.

Data from lidar, DWM node and inertial sensors are synchronized with each other by the corresponding timestamps. For the filtration of UWB measurements data from inertial sensors were used. Data from the UWB system are burdened with an error that depends on the distance between two network nodes and the place of attachment on the vehicle (the distance between the node and the surface on which the object moves is the most influential one).

Additional static tests (in addition to the dynamic tests described in the section "B. Test scenarios") were performed to determine the error value which depends on the distance between the nodes. On the tripods, two UWB nodes were hanged opposite to each other at the height of 150 cm. The tests were carried out indoors and outdoors at the following distances: 0.25 m, 0.5 m, 0.75 m, 1 m, 1.5 m, 2 m, 3 m, 4 m, 5 m, 6 m, 8 m, 10 m, 15 m, 20 m, 25 m, 30 and additionally outdoors at 40 m and 44 m.

Each measurement series (reference distance) contains 10 000 samples.

The results of static measurements are shown separately for indoor (Fig. 7) and outdoor (Fig. 8) environments. The graphs also show the change in error depending on the distance. Negative error values mean underestimation, and positive values mean overestimation of the distance.

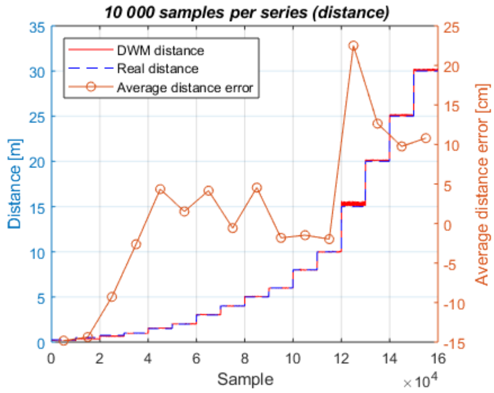

Fig. 7. Average distance error for static measurements inside building.

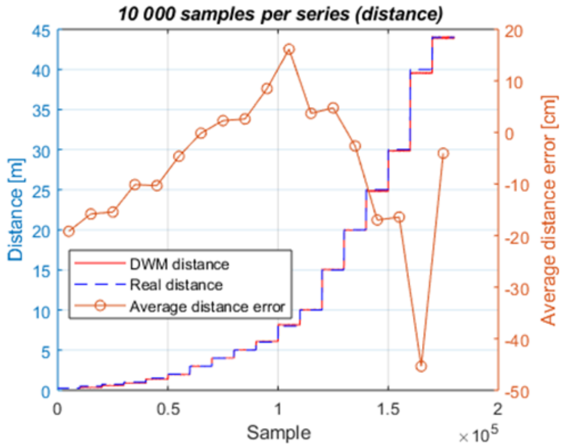

Fig. 8. Average distance error for static measurements outside building.

Table I summarizes (for measurements inside and outside the building) the average error obtained in static measurements.

TABLE I: AVERAGE DISTANCE ERROR FOR STATIC MEASUREMENTS INDOORS AND OUTDOORS

Reference distance [m]	Indoor [cm]	Outdoor [cm]
0.25	-14.82	-19.18
0.5	-14.36	-15.81
0.75	-9.28	-15.44
1	-2.62	-10.12
1.5	4.35	-10.32
2	1.52	-4.64
3	4.16	-0.14
4	-0.58	2.29
5	4.54	2.62
6	-1.81	8.51
8	-1.48	16.15
10	-1.97	3.70
15	22.51	4.76
20	12.64	-2.63
25	9.75	-16.98
30	10.80	-16.43
40	-	-45.35
44	-	-4.05

Based on the calculated distance errors, the square function was fitted (data in mm was used to fit the function – which is important to appraise the obtained coefficients of the function). To obtain the most universal function, the fitting was carried out at once on the data obtained outside and inside the building – see Fig. 9. The function value specifies the value of the distance correction factor – α

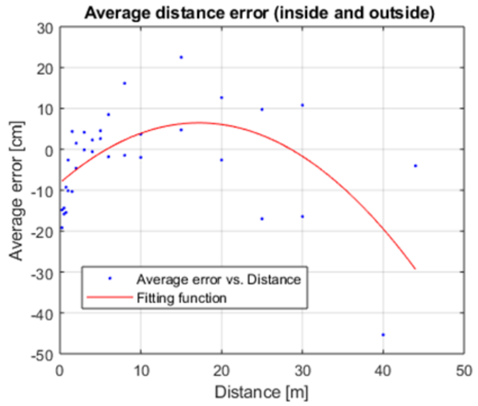

Fig. 9. Square function fitting.

The used function – the polynomial of degree 2 (2), allows to show the distance error changes really well, while maintaining low computational complexity, which, in turn, is important when filtering data in real time.

$$\alpha_i = a_1 \cdot d_{UWB}^2 + a_2 \cdot d_{UWB} + a_3 \qquad (2)$$

where: a_1, a_2 and a_3 – function coefficients, d_{UWB} – distance from UWB system.

The quadratic function with the following coefficients was obtained (the root mean square error (RMSE) of the fit is 10.7 cm):

- $a_1 = -4.98 \cdot 10^{-7}$
- $a_2 = 1.71 \cdot 10^{-2}$
- $a_3 = -82.04$

Using the calculated correction factor, it is possible to perform distance adjustment on the data from UWB (3).

$$d_{i_{UWB_A}} = d_{i_{UWB}} - \alpha_i - \beta \qquad (3)$$

where: d_{iUWB} – i-th distance from UWB system; α_i – correction factor for i-th distance; β – mounting correction factor.

Accelerometer data allow to determine the type of the movement of the vehicle. For this purpose a linear regression is determined in a window of 3 samples and the angle of slope of this function is examined. In the next step it is checked if the calculated angle is in the range ⟨-γ; γ⟩, which determines the system noise. If the noise is detected, it means that the acceleration should be 0 m/s^2, otherwise the accelerometer data stay unchanged.

For the purpose of this study, three states of vehicle movement were identified as follows:

- Vehicle has not started moving – a start sequence is expected. Accelerations will exceed the γ_{start} threshold in the sequence;

- Vehicle is moving – after detecting the start sequence, the vehicle is moving, a braking sequence is expected where acceleration will exceed the γ_{stop} threshold. Data from UWB system are filtered. The average distance in the window of 5 samples and the maximum displacement based on the current speed and the average value of previous sample are tested. If the filtered value in the window and the average value differ from each other by more than the maximum possible displacement, the new value is the sum of the previous average value and the maximum displacement, otherwise the new value is the average value;
- Vehicle stopped – after detecting the braking series, a sequence indicating that the vehicle is not moving is expected (no acceleration in the accelerometer indications);

IV. Test Result

Data from UWB system which are not analyzed and corrected are characterized by a relatively large error. Table II represents the average absolute error (AAE) and RMSE of distances for smooth traffic and with stops inside and outside environment. The RMSE indoor is, on average, larger by more than 11 cm than outdoors – see Table III. In addition, the error inside building in the passage with stops is higher than in smooth traffic. This is due to the nature of the room – a narrow corridor with a large number of recesses and doors which cause interference and reflection of the UWB signal.

TABLE II: Distance Error – Raw Data

Environment	Passage	Distance error [cm]	
		AAE	RMSE
Indoor	Smooth	26.30	28.92
	Start-stop	34.55	37.75
Outdoor	Smooth	21.33	21.89
	Start-stop	21.42	21.85

TABLE III: Average Distance Error – Raw Data

Environment	Average distance error [cm]	
	AAE	RMSE
Indoor	30.15	33.04
Outdoor	21.37	21.87
In/Outdoor avg	**26.44**	**28.32**

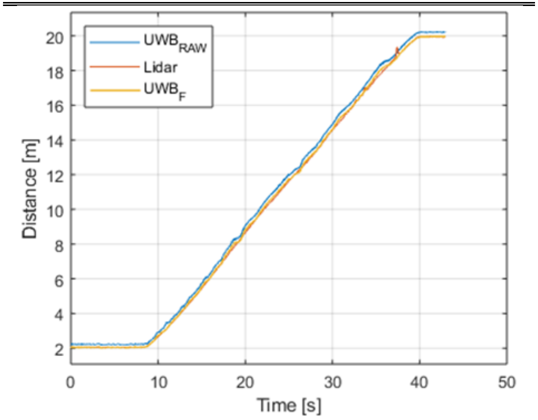

Fig. 10. Example of smooth passage inside building.

Fig. 10 shows an example of a smooth passage inside the building. The vehicle started to move 2 m from the reference point and moved away from it. You can clearly notice the data shift which is removed at the stage of data correction process. In addition, the UWB data were filtered based on data from the accelerometer, which led to smoothing the data while maintaining the sharpness of the waveform – see Fig. 11.

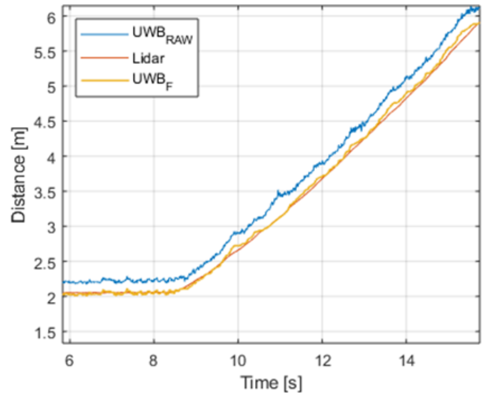

Fig. 11. The effect of data filtration for smooth passage – indoor.

Fig. 12 shows an example of a start-stop passage inside the building. After the correction and filtration process, the data more accurately reflect the reference passage. The sharpness is maintained – see Fig. 13.

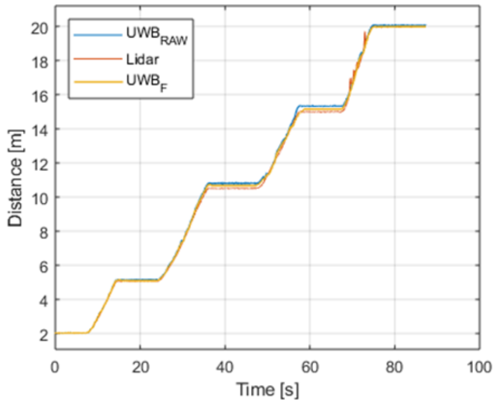

Fig. 12. Example of start-stop passage inside building.

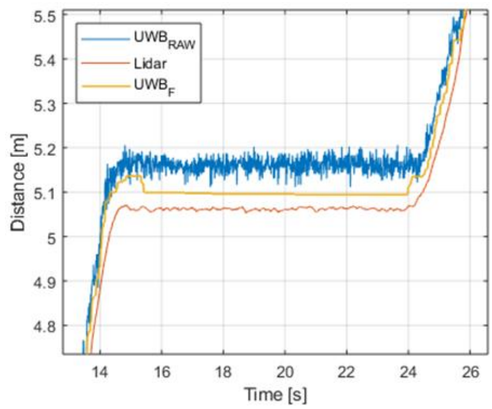

Fig. 13. The effect of data filtration for start-stop passage – indoor.

Improvement is also noted for outdoor movements. An example of a start-stop passage is shown in Fig. 14. UWB data are highly filtered – the system noise is removed.

UWB data correction and filtration greatly improve the ranging result (see Table IV) and average values for both types of passage in Table V. Looking at RMSE, distance measurement inside the building improved by over 16 cm for smooth traffic and by over 17 cm for traffic with stops. In the outside environment, there was also an increase in accuracy. For the smooth passage, the ranging error was reduced by almost 13 cm, while for the start-stop passage by more than 13 cm.

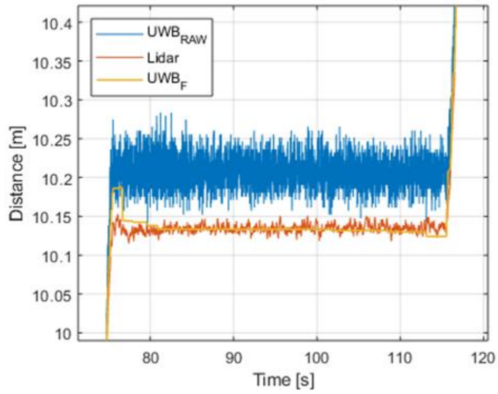

Fig. 14. The effect of data filtration for start-stop passage – outdoor.

TABLE IV: DISTANCE ERROR – DATA AFTER CORRECTION AND FILTRATION

Environment	Passage	Distance error [cm]	
		AAE	RMSE
Indoor	Smooth	9.27	12.82
	Start-stop	12.96	20.52
Outdoor	Smooth	7.67	9.11
	Start-stop	7.53	8.69

TABLE V: AVERAGE DISTANCE ERROR - DATA AFTER CORRECTION AND FILTRATION

Environment	Average distance error [cm]	
	AAE	RMSE
Indoor	10.99	16.42
Outdoor	7.61	8.92
In/Outdoor avg	**9.56**	**13.24**

V. CONCLUSION

The UWB system is a good complement to the GPS system inside buildings where the GPS system does not provide useful information (because of weak or lack of a signal) or in places where high accuracy of the determined position is required. The raw distances are burdened with 22 cm outdoor and 33 cm indoor errors (RMSE). The presented correction and filtration process improves the accuracy of the distance determination between two UWB nodes. The UWB system after the correction and filtration process is characterized by an accuracy (RMSE) of 9 cm outdoors (improved by 59% compared to raw data), and an accuracy of 16 cm indoors (improved by 50% compared to raw data) during the movement of the localized object. The presented methods increased the ranging accuracy both for indoor and outdoor environment by more than twice (on average improved by 53% compared to raw data).

Integrating UWB system with inertial navigation system has a positive effect on the ranging accuracy. Recognition of the state of the localized object is a key to applying the appropriate method of data filtration. The fusion of data from the INS and UWB systems eliminates random errors and gives possibility to determine the maximum difference between successive samples.

CONFLICT OF INTEREST

The authors declare no conflict of interest.

AUTHOR CONTRIBUTIONS

Tomczyk, Marciniak conducted the research; Paszek analyzed the data and wrote the paper; Grzechca supervised the research; all authors had approved the final version.

REFERENCES

[1] A. Alarifi, *et al*., "Ultra wideband indoor positioning technologies: Analysis and recent advances," *Sensors*, vol. 16, no. 5, p. 707, May 2016.

[2] M. Matosevic, Z. Salcic, and S. Berber, "A Comparison of accuracy using a GPS and a low-cost DGPS," *IEEE Trans. Instrum. Meas.*, vol. 55, no. 5, pp. 1677-1683, Oct. 2006.

[3] H. Qi and J. B. Moore, "Direct Kalman filtering approach for GPS/INS integration," *IEEE Trans. Aerosp. Electron. Syst*., vol. 38, no. 2, pp. 687-693, Apr. 2002.

[4] H. Deilamsalehy and T. C. Havens, "Sensor fused three-dimensional localization using IMU, camera and LiDAR," in *Proc. IEEE SENSORS*, Orlando, FL, USA, 2016, pp. 1-3.

[5] J. Wei, J. M. Snider, J. Kim, J. M. Dolan, R. Rajkumar, and B. Litkouhi, "Towards a viable autonomous driving research platform," in *Proc. IEEE Intelligent Vehicles Symposium (IV)*, Gold Coast City, Australia, 2013, pp. 763-770.

[6] T. Ogawa, H. Sakai, Y. Suzuki, K. Takagi, and K. Morikawa, "Pedestrian detection and tracking using in-vehicle lidar for automotive application," in *Proc. IEEE Intelligent Vehicles Symposium (IV)*, Baden-Baden, Germany, 2011, pp. 734-739.

[7] C. Deng, S. Wang, J. Liu, and Z. Yu, "A novel intelligent working monitoring and guarding system of smart substations based on UWB positioning and aerial LiDAR data," *J. Commun.*, vol. 11, no. 8, pp. 765-771, 2016.

[8] H. Rohling, S. Heuel, and H. Ritter, "Pedestrian detection procedure integrated into an 24 GHz automotive radar," in *Proc. IEEE Radar Conference*, Arlington, VA, USA, 2010, pp. 1229-1232.

[9] A. Bose and C. H. Foh, "A practical path loss model for indoor WiFi positioning enhancement," in *Proc. 6th International Conference on Information, Communications & Signal Processing*, 2007, pp. 1-5.

[10] Y. Gu and F. Ren, "Energy-efficient indoor localization of smart hand-held devices using Bluetooth," *IEEE Access*, vol. 3, pp. 1450-1461, 2015.

[11] H. J. Chu, G. J. Tsai, K. W. Chiang, and T. T. Duong, "GPS/MEMS INS data fusion and map matching in urban

areas," *Sensors*, vol. 13, no. 9, pp. 11280-11288, Aug. 2013.

[12] H. Hellmers, A. Eichhorn, A. Norrdine, and J. Blankenbach, "Indoor localisation for wheeled platforms based on IMU and artificially generated magnetic field," in *Proc. Ubiquitous Positioning Indoor Navigation and Location Based Service (UPINLBS)*, Corpus Christ, TX, USA, 2014, pp. 255-264.

[13] A. Ziebinski, R. Cupek, H. Erdogan, and S. Waechter, "A survey of ADAS technologies for the future perspective of sensor fusion," in *Computational Collective Intelligence*, vol. 9876, N. T. Nguyen, L. Iliadis, Y. Manolopoulos, and B. Trawiński, Eds. Cham: Springer International Publishing, 2016, pp. 135-146.

[14] J. Miura, T. Kanda, and Y. Shirai, "An active vision system for real-time traffic sign recognition," in *Proc. IEEE Intelligent Transportation Systems*, 2000, pp. 52-57.

[15] L. Xiao and F. Gao, "A comprehensive review of the development of adaptive cruise control systems," *Veh. Syst. Dyn.*, vol. 48, no. 10, pp. 1167-1192, Oct. 2010.

[16] Abdulhakam, A. M. Assidiq, O. O. Khalifa, M. R. Islam, and S. Khan, "Real time lane detection for autonomous vehicles," in *Proc. International Conference on Computer and Communication Engineering*, Kuala Lumpur, Malaysia, 2008, pp. 82-88.

[17] R. Toledo-Moreo, D. Betaille, F. Peyret, and J. Laneurit, "Fusing GNSS, dead-reckoning, and enhanced maps for road vehicle lane-level navigation," *IEEE J. Sel. Top. Signal Process.*, vol. 3, no. 5, pp. 798-809, Oct. 2009.

[18] C. Lian Sang, M. Adams, T. Hörmann, M. Hesse, M. Porrmann, and U. Rückert, "Numerical and experimental evaluation of error estimation for two-way ranging methods," *Sensors*, vol. 19, no. 3, pp. 616, Feb. 2019.

[19] R. Misra, S. Shukla, and V. Chandel, "Lightweight localization using trilateration for sensor networks," *Int. J. Wirel. Inf. Netw.*, vol. 21, no. 2, pp. 89-100, Jun. 2014.

[20] G. Schroeer, "A real-time UWB multi-channel indoor positioning system for industrial scenarios," in *Proc. International Conference on Indoor Positioning and Indoor Navigation (IPIN)*, Nantes, 2018, pp. 1-5.

[21] A. R. J. Ruiz and F. S. Granja, "Comparing ubisense, BeSpoon, and DecaWave UWB location systems: Indoor performance analysis," *IEEE Trans. Instrum. Meas.*, vol. 66, no. 8, pp. 2106-2117, Aug. 2017.

[22] Decawave, DW1000 User Manual. (2017). [Online]. Available:https://www.decawave.com/sites/default/files/resources/dw1000_user_manual_2.11.pdf.

[23] M. D. Oliveira, N. Araujo, R. D. Silva, T. D. Silva, and J. Epaarachchi, "Use of Savitzky–Golay filter for performances improvement of SHM systems based on neural networks and distributed PZT sensors," *Sensors*, vol. 18, no. 2, pp. 152, Jan. 2018.

Krzysztof Paszek was born in Mikołów, Silesia Poland in 1992. He received the B.S. and M.S. degrees in informatics from the Faculty of Automatic Control, Electronics and Computer Science of Silesian University of Technology, Gliwice, in 2017.
From 2017, he is a regular Ph.D. student and from the 2018 student of Cyber-physical system studies on Faculty of Automatic Control, Electronics and Computer Science of Silesian University of Technology, Gliwice. His research interest includes the data analysis, objects positioning, advanced driver-assistance systems, data fusion and machine learning.

Damian E. Grzechca (M'03-SM'13) received MSc, PhD and DSc. from the Institute of Electronics, Silesian University of Technology, Gliwice, Poland in 1998, 2003 and 2013, respectively. He is interested in artificial intelligence methods to engineering problems i.e. test and diagnosis of analog and mixed-signal electronic circuits, enhance adaptive driver assistance systems, localization and positioning of objects. He cooperates with industry and creates innovative test solutions for Automotive like TPMS and PEPS testers, aging analysis for rail electronic modules. His current research concerns data fusion for various aspects of car perception e.g. adaptive cruise control in smart city environment. He has been a visiting researcher at the Bournemouth University, UK and TIMA laboratory in Grenoble, France. He is an author co-author of more than 100 scientific papers, a supervisor of Project Based Learning module for the best students. He introduced a number of courses for undergraduate students on a distance learning platform, e.g. fundamental of electric and electronic circuits, signal processing and real time locating systems.

Mateusz Tomczyk received B.S. in information and communication technology from the Faculty of Automatic Control, Electronics and Computer Science of Silesian University of Technology, Gliwice in 2018. Currently he is studying informatics on Faculty of Automatic Control, Electronics and Computer Science of Silesian University of Technology, Gliwice. He is interested in system software, MEMS, wireless communication systems, positioning and data transfer using wireless technology such as UWB.

Artur Marciniak received B.S. in information and communication technology from the Faculty of Automatic Control, Electronics and Computer Science of Silesian University of Technology, Gliwice in 2018. Currently he is studying informatics on Faculty of Automatic Control,

Electronics and Computer Science of Silesian University of Technology, Gliwice. He is interested in system software, IoT technology, various sensors systems, and positioning using wireless technology such as UWB assisted by other systems.